MDPI

Article

Raman Spectroscopy diagnosis of Melanoma

Gianmarco Lazzini [1,2], Daniela Massi [3], Davide Moroni [1]*, Ovidio Salvetti [1], Paolo Viacava[4], Marco Laurino[5], and Mario D'Acunto[2]

[1] CNR-ISTI, National Research Council, via Moruzzi 1, 56124, Pisa, Italy
[2] CNR-IBF, Institute of Biophysics, National Research Council, via Moruzzi 1, 56124, Pisa, Italy
[3] Section of Pathological Anatomy, Dept of Health Sciences, University of Florence; Florence, Italy
[4] Unit of Dermatology, Specialist Surgery Area, Department of General Surgery, Livorno Hospital, Azienda Usl Toscana Nord Ovest, Livorno, Ital
[5] CNR-IFC, Institute of Clinical Physiology, National Research Council, 56124, Pisa, Italy
* Correspondence: davide.moroni@isti.cnr.it

Abstract: Cutaneous melanoma is an aggressive form of skin cancer and a leading cause of cancer-related mortality. In this sense, Raman Spectroscopy (RS) could represent a fast and effective method for melanoma-related diagnosis. We therefore introduced a new method based on RS to distinguish Compound Naevi (CN) from Primary Cutaneous Melanoma (PCM) from *ex vivo* solid biopsies. To this aim, integrating Confocal Raman Micro-Spectroscopy (CRM) with four Machine Learning (ML) algorithms: Linear Discriminant Analysis (LDA), Quadratic Discriminant Analysis (QDA), Support Vector Machine (SVM), and Random Forest Classifier (RFC). We focused our attention on the comparison between traditional pre-processing operations with Continuous Wavelet Transform (CWT). In particular, CWT led to the maximum classification accuracy, which was of ∼89.0%, which highlighted the method as promising in view of future implementations in devices for everyday use.

Keywords: Raman, Melanoma, Machine Learning, Continuous Wavelet Transform

1. Introduction

Among the skin cancers, Cutaneous Melanoma (CM) turns out to be the most aggressive and mortal form [1]. Today, the most accepted method for CM diagnosis is represented by a dermoscopy-assisted clinical examination, followed by a histopathological assessment [2]. These operations show several drawbacks, including the high percentage of false positive cases after the initial examination, or strong similarities between histotypes of different nature. Raman Spectroscopy (RS) has emerged as a highly promising technique to address the aforementioned issues. This method measures the so-called Raman effect [3]. RS potentially allows the distinction between complex samples that appear macroscopically identical. In contrast to the conventional histopathological examination,RS can identify melanoma within minutes [4]. Finally, due to its label-free character, RS is suitable either for *ex vivo* or *in vivo* measurements. However, the large amount of information within a single Raman spectrum hinders the qualitative interpretation of such experimental data. In this sense, Machine Learning (ML) represents a complementary tool to rapidly read and elaborate Raman data, to bring out the information of interest. In this paper, we built an innovative approach, based on the coupling between Confocal Raman Microscopy (CRM) and ML, i.e., Linear Discriminant Analysis (LDA), Quadratic Discriminant Analysis (QDA), Support Vector Machine (SVM), and Random Forest Classifier (RFC), as a diagnostic tool to distinguish solid biopsies of Compound Naevus (CN) and Primary Cutaneous Melanoma

Received:
Revised:
Accepted:
Published:

Citation: . Raman Spectroscopy diagnosis of Melanoma. *Journal Not Specified* **2025**, *1*, 0. https://doi.org/

(PCM). We explored two different approaches for the spectral pre-processing: the conventional techniques, based on the fluorescence (baseline) removal, and the Continuous Wavelet Transform (CWT), which allowed to deconvolve the baseline from the Raman component. This last solution led to a significant increase in the classification accuracy, which reached the maximum value of $\sim 89\%$ for RFC.

2. Materials and Methods

The study involved 5μm-thick Formalin-fixed paraffin-embedded (FFPE) tissue sections of CN (12 biopsies) and PCM (18 biopsies), retrospectively retrieved from the Section of Pathology at the Department of Health Sciences, University of Florence, and from the Azienda USL Nord-Ovest Toscana, Livorno, Italy. We collected spectra in grids of resolution 25μm$\times$25μm within the cutaneous lesions. A single spectrum was the result of the arithmetic mean of 85 accumulations, with an acquisition time of 0.2 s per accumulation. In addition, we restricted our analysis to the spectral interval between 400 and 1800 cm^{-1}. We retrieved between 150 and 200 spectra per biopsy, depending on the amount of tissue available. To suppress effects related to spatial non-uniformities (voids or cracks), we normalized the raw spectra by the integral value. In this study, we compared two different pre-processing approaches: in one case, we removed the baseline, attributed to sample fluorescence, through an Asymmetrically Reweighted Penalized Least Squares (ARPLS) algorithm [5]. Subsequently, we suppressed the high-frequency noise with a Savitzky-Golay (SG) algorithm (window: 17 points; polynomial order: 3). In a second approach, we applied the Continuous Wavelet Transform (CWT) [6]. This operation can be conceived as the convolution of the original signal $x(t)$ with a series of wavelets $\{\Psi\left(\frac{t-b}{a}\right)\}$, where b is a traslational parameter and $a > 0$ is called scale. The aforementioned wavelets are generated from the so-called mother wavelet $\Psi(t)$. In this work, we adopted the so-called "Mexican hat" as the mother wavelet [7]. In addition, we adopted an array of $N_s = 100$ evenly spaced scales between 0.1 and 100. When applied to a single Raman spectrum, CWT led to a vector of $N_s \times N_p = 69300$ components, where N_p is the number of components of the original spectrum. As we will explain in detail in the following, we focused our attention on the problem of distinguishing CN and PCM. Since the number of biopsies and, consequently, the number of spectra of CN and PCM was not the same, after having performed the pre-processing operations, we applied a Synthetic Minority Oversampling TEchnique (SMOTE) to obtain a balanced dataset of $N_{spectra} = 5100$ spectra [8]. Finally, we applied PCA to the resulting spectra to reduce the system dimensionality, and employed the first $N_{PCA} = 10$ Principal Components (PCs) to feed the ML models. We tested the classification performances of LDA, QDA, SVM (kernel: radial basis function, RBF), and RFC. In particular, in SVM, we fixed the γ parameter of RBF to N_{PCA}^{-1} and optimized the regularization parameter C based on the maximization of the classification accuracy through a grid-like procedure employing an array of evenly speced values of C between 10^{-1} and 5. Finally, in RFC, the trees of the forest were grown until reaching 100% training accuracy, and each tree node was obtained by randomly choosing $N_p^{\frac{1}{2}}$ among the features available in the dataset and by selecting the feature leading to the maximum gain in terms of Gini index. To build the whole forest, we optimized the number N_t of trees through a grid-like procedure, adopting an array of evenly spaced integers between 50 and 150. We quantified the classification performances with a 10-Fold Cross-validation, in terms of Accuracy (A), Area Under ROC curve (AUROC), Recall (R), and Precision (P).

3. Results

In Fig. 1 we reported the averaged Raman signal associated with PCM and CN. The most relevant detail observable from the qualitative analysis of this graph is the strong

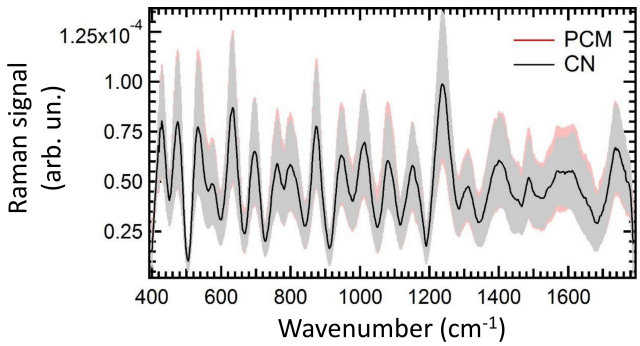

Figure 1. Averaged RS of PCM (red) and CN (black). Shaded areas represent the standard deviation.

overlap between the two signals, as testified by the averaged signal and the corresponding standard deviation, which is represented here as shaded areas. This outcome can be seen as further proof of the inadequacy of a qualitative approach aimed at distinguishing the two classes, CN and PCM. The lack of distinct spectral bands with significant intensity differences between CN and PCM indicates that a machine learning (ML) model's classification power must depend on the combined statistical data from multiple spectral components. This suggests that highly non-linear ML models are the best candidates for high classification accuracy. This conclusion is supported by the performance of the models in this study. Linear models like LDA, QDA, and SVM performed similarly, with accuracies too low for reliability. In contrast, the highly non-linear Random Forest Classifier (RFC) achieved the best results, with accuracy reaching approximately 80-89

Table 1. Classification performances of the ML classifiers, for the two pre-processing conditions examined. Errors are determined as the standard deviation on the folds of the Cross-Validation.

Classifier	**Pre-processing**	A **(%)**	$AUROC$ **(%)**	R **(%)**	P **(%)**
LDA	CWT	63.2 ± 2.6	67.3 ± 3.6	63.2 ± 2.6	63.2 ± 2.5
LDA	ARPLS+SG	63.0 ± 2.6	65.1 ± 2.7	63.0 ± 2.6	63.4 ± 2.7
QDA	CWT	55.0 ± 3.2	55.3 ± 4.9	55.0 ± 3.2	58.2 ± 5.1
QDA	ARPLS+SG	49.9 ± 0.1	50.0 ± 0.1	49.9 ± 0.1	24.9 ± 0.1
SVM	CWT	55.8 ± 3.5	66.3 ± 4.1	55.8 ± 3.4	61.3 ± 6.1
SVM	ARPLS+SG	49.9 ± 0.1	60.9 ± 3.9	49.9 ± 0.1	24.9 ± 0.1
RFC	CWT	89.1 ± 1.7	96.0 ± 1.1	$89.1.8 \pm 1.7$	89.1 ± 1.7
RFC	ARPLS+SG	79.6 ± 1.9	87.9 ± 1.3	79.6 ± 1.9	79.7 ± 1.9

The second interesting outcome of this analysis comes from the comparison between the two pre-processing conditions adopted in this paper. The conventional condition ARPLS+SG, based on the baseline removal, led to the worst classification performances, probably indicating that the baseline component, attributable to the sample fluorescence, contains precious information for the correct classification. On the other hand, CWT, which doesn't involve signal removal, allows for maintaining the baseline contribution, resulting in better performance. Despite this interesting result, CWT led to the drawback of dramatically increasing the number of features employed to feed the ML models. Although this effect can be attenuated by applying PCA, it turns out to be time-consuming, with potential negative consequences in terms of practical use and/or the occurrence of overfitting. In our case, while ARPLS+SG required $\sim$ 10 s to be accomplished, CWT required $\sim$ 59 s. This aspect must be taken into account in view of the future applications of this technology in

engineered devices, where requirements such as high diagnostic speed and reliability are mandatory.

4. Conclusions

In this preliminary investigation, we explored the possibility of employing the Confocal Raman Microscopy coupled with Machine Learning to diagnose Cutaneous Melanoma from solid biopsies, i.e., to distinguish Primary Cutaneous Melanoma from Compound Naevus. To this aim, we employed the resulting Raman spectra as examples to build ML models based on different principles. Furthermore, we compared the traditional preprocessing operations, based on the removal of the baseline filtering, with an innovative approach, i.e., the application of the Continuous Wavelet transform (CWT). The results of such an investigation highlighted how Random Forest Classifier led to the maximum classification accuracy, with values reaching $\sim 89\%$, acting as a good candidate for future employments in engineered devices. Among the most promising routes, we mention the employment in an *ex vivo* fashion to assist the histopathologists during the diagnostic process, or for the realization of probes for non-invasive *in vivo* diagnosis. Finally, the classification performances were maximized with CWT, indicating that the signal baseline, usually considered an undesired contribution to the measured signal, carries valuable information for the diagnostic task.

Funding: This research was funded by the Regione Toscana through the TELEMO Project under Grant Ricerca Salute 2018

Institutional Review Board Statement: The study was conducted in accordance with the Declaration of Helsinki, and approved by the Institutional Review Board of Azienda USL Toscana Nord Ovest U.O.C. Dermatologia - Livorno Mod. PROTOCOLLO STUDIO PILOTA OSSERVAZIONALE B11 Vers_20160118.

Informed Consent Statement: Informed consent was obtained from all subjects involved in the study.

Conflicts of Interest: The authors declare no conflict of interest.

References

1. Saginala, K.; Barsouk, A.; Aluru, J.S.; Rawla, P.; Barsouk, A. Epidemiology of melanoma. *Medical sciences* **2021**, *9*, 63.
2. Senan, E.M.; Jadhav, M.E. Analysis of dermoscopy images by using ABCD rule for early detection of skin cancer. *Global Transitions Proceedings* **2021**, *2*, 1–7.
3. Raman, C.V.; Krishnan, K.S. A new type of secondary radiation. *Nature* **1928**, *121*, 501–502.
4. Fox, S.A.; Shanblatt, A.A.; Beckman, H.; Strasswimmer, J.; Terentis, A.C. Raman spectroscopy differentiates squamous cell carcinoma (SCC) from normal skin following treatment with a high-powered CO2 laser. *Lasers in Surg. Med.* **2014**, *46*, 757–772.
5. Baek, S.J.; Park, A.; Ahn, Y.J.; Choo, J. Baseline correction using asymmetrically reweighted penalized least squares smoothing. *Analyst* **2015**, *140*, 250–257.
6. Kandjani, A.E.; Griffin, M.J.; Ramanathan, R.; Ippolito, S.J.; Bhargava, S.K.; Bansal, V. A new paradigm for signal processing of Raman spectra using a smoothing free algorithm: Coupling continuous wavelet transform with signal removal method. *J. of Raman Spect.* **2013**, *44*, 608–621.
7. Ramakrishnan, S. Introductory Chapter: Wavelet Theory and Modern Applications. In *Modern Applications of Wavelet Transform*; IntechOpen, 2024.
8. Bellantuono, L. Artificial Intelligence-assisted thyroid cancer diagnosis from Raman spectra of histological samples. *IL NUOVO CIMENTO* **2024**, *100*, 47.